Charged- and neutral-current solar-neutrino cross sections for heavy-water Cherenkov detectors

S. Ying, W. C. Haxton, and E. M. Henley
Department of Physics, FM-15, and National Institute for Nuclear Theory, HN-12, University of Washington, Seattle, Washington 98195
(Received 26 December 1991)

Charged- and neutral-current neutrino cross sections for deuterium have been calculated for the Bonn, Paris, and Hamada-Johnson potentials in order to estimate event rates (and their uncertainties) for solar and supernova neutrino detection in the Sudbury Solar Neutrino Observatory. Tests of the wave functions are provided by calculations of the $j=\frac{1}{2}$ hyperfine-state muon capture rate and of the total cross section for absorbing $\nu_e s$ from stopped muon decay. Detailed tables of the Paris potential results are given, and comparisons are made to the work of Doi and Kubodera.

PACS number(s): 25.30.Pt, 96.60.Kx, 95.30.Cq

The Sudbury Neutrino Observatory (SNO) Collaboration [1] is constructing a 1-ktonne heavy-water Cherenkov detector to record the charged-current and neutral-current interactions of solar and supernova neutrinos. The high event rate for $\nu_e+d \to e^- + p + p$ combined with the low threshold of the SNO detector, ~ 5 MeV, may allow the experimenters to reconstruct the shape of the high-energy portion of the ^{8}B neutrino spectrum. The neutral-current reaction $\nu+d \to \nu + n + p$, where the neutron is detected by its capture γ rays, is sensitive to neutrinos of any flavor. Both of these reactions could help establish whether matter-enhanced neutrino oscillations are responsible for the solar-neutrino puzzle: the detection of solar muon or tauon neutrinos or a ν_e spectral shape characteristic of Mikheyev-Smirnov-Wolfenstein (MSW) oscillations [2] would signify new particle physics.

A number of authors estimated the cross sections for neutral- and charged-current breakup of the deuteron in an approximation where the final two-nucleon state is in a relative s wave, and the weak operators are evaluated in the allowed approximation [3]. However, the SNO detector will also serve as an important observatory for the $\nu_e s$, $\nu_\mu s$, and $\nu_\tau s$ emitted by galactic supernovae. Supernova models predict that the spectra of $\nu_\mu s$ and $\nu_\tau s$ will be characterized by mean energies of 25–30 MeV and will have tails that extend to much higher energies [4]. It was argued by Ying, Haxton, and Henley (YHH) [5] that first-forbidden contributions could become important at the higher energies, requiring a more careful treatment of the final nuclear state. In YHH we reevaluated the weak cross sections, retaining the full one-body weak interaction, rather than just the allowed operators, and all final-state partial waves that these operators could excite.

Subsequently a similar calculation was performed by Tatara, Kohyama, and Kubodera (TKK) [6]. There were significant differences in the two approaches: TKK included a full set of exchange current corrections, and used the convection current form of the vector $E1$ operator rather than the Siegert's theorem expression. They did not include terms proportional to the square of the vector three-current (e.g., $|E1^V|^2$ and $|M1^V|^2$). The two calculations agree for low neutrino energies, but seriously disagree away from threshold, indicating a substantial difference in the treatment of the first-forbidden response. *A priori* it was not clear whether the discrepancy was due to a numerical problem, or to one or more of the technical differences mentioned above.

In the present paper and in the accompanying paper by Doi and Kubodera [7] the discrepancy is almost entirely resolved. Most of the discrepancy is attributable to a coding error in one of the first-forbidden matrix elements of YHH, leading to a cross section that rises too steeply with neutrino energy, as described below. The error introduced is more than a factor of 2 for $E_\nu \gtrsim 100$ MeV. Also, the inclusion of a full set of vector multipoles by Doi and Kubodera leads to an increase of about 30% in the higher-energy ($E_\nu \sim 150$ MeV) results of TKK. As a result of these changes, the results of the present paper and those of Doi and Kubodera are generally in accord at the 5% level of accuracy, suggesting that the various breakup cross sections are now very well understood.

The differences between our present calculations and those of YHH are as follows: (1) The first-forbidden matrix element arising from the $J=1$ magnetic projection of the axial-vector current was too large in our earlier work because of a factor of 2 coding error in this amplitude. This is corrected in the present work. (2) The q^2 dependence of single-nucleon form factors F_1, F_2, and F_A (see Eqs. (2.7) of Ref. [5]) is now retained. (3) Calculations of $j=\frac{1}{2}$ hyperfine-state muon-capture rate and the total neutrino reaction cross section for $\nu_e s$ from stopped muon decay have been completed. Although the former depends on the pseudoscalar coupling F_P, a parameter that is somewhat uncertain in nuclei, the resulting comparisons with experiment do provide important tests of our wave functions at momentum transfers typical of supernova neutrino reactions. (4) The accompanying paper by Doi and Kubodera presents an independent estimate of the relevant neutrino cross sections. The comparison of the two calculations provides a measure of the theoretical uncertainties associated with different strong potentials, alternative prescriptions for imposing the constraints of current conservation, and meson exchange currents. We find that the ratios of the Doi and Kubodera charged- and neutral-current cross sections to those we evaluate here range from 1.00 to 1.18 over the region from threshold to 150 MeV, with the agreement better than 5% for all but the very lowest energies.

The technical details of the calculations follow Ref. [5]. The charged current has the form

$$J_\mu^\pm = V_\mu^\pm + A_\mu^\pm \ , \tag{1}$$

where V_μ and A_μ denote the vector and axial-vector currents, respectively. The standard-model neutral current is

$$J_\mu^{\rm NC} = -2\sin^2\theta_W V_\mu^S + (1-2\sin^2\theta_W)V_\mu^3 + A_\mu^3 \ , \tag{2}$$

where V_μ^s is the isoscalar part of the vector (electromagnetic) current, and V_μ^3 and A_μ^3 are the third components of the isovector currents appearing in (1). The nuclear operators are derived by completing a Pauli expansion of the on-shell nucleon matrix elements of these currents

$$\langle N'|V_\mu^\pm|N\rangle = \bar{u}(p')\left[F_1^V\gamma_\mu + iF_2^V\sigma_{\mu\nu}\frac{q^\nu}{2M}\right]\tau_\pm u(p) \ , \tag{3a}$$

$$\langle N'|A_\mu^\pm|N\rangle = \bar{u}(p')(F_A\gamma_\mu\gamma_5 + F_P\gamma_5 q_\mu)\tau_\pm u(p) \tag{3b}$$

to order $1/M$. We define $q_\mu = (p'-p)_\mu$ and $q^2 = q_0^2 - \mathbf{q}^2$. The isovector form factors have the $q^2=0$ values $F_1^V(0)=1$, $F_2^V(0)=\mu_p-\mu_n=3.706$, and $F_A(0)=-1.254$, and their q^2 dependence is taken to be

$$F(q^2) = F(0)/[1-q^2/(0.71\ \text{GeV}^2)]^2 \ . \tag{4}$$

The pseudoscalar form factor is given by pion-pole dominance

$$F_P(q^2) = -\frac{2MF_A(0)}{q^2-m_\pi^2} \ .$$

The isovector neutral-current matrix elements are obtained by replacing $\tau_\pm$ by $\tau_3/2$ in Eqs. (3), while the isoscalar vector current matrix element is

$$\langle N'|V_\mu^S|N\rangle = \bar{u}(p')(F_1^S\gamma_\mu + iF_2^S\sigma_{\mu\nu}q^\nu)\frac{\tau_3}{2}u(p) \ ,$$

where $F_1^S(0)=1$ and $F_2^S(0)=\mu_p+\mu_n=-0.120$.

A standard multipole analysis yields double differential cross sections $d^2\sigma/d\omega\, d\Omega$, where Ω is the scattering an-

TABLE I. Total Paris potential neutral-current and charged-current cross sections for the breakup of deuterium as a function of the incident neutrino energy. The units are 10^{-42} cm^2, and $(-x)$ denotes 10^{-x}.

E_ν (MeV)	$\nu+d\to\nu'+n+p$	$\bar\nu+d\to\bar\nu'+n+p$	$\nu+d\to e^-+p+p$	$\bar\nu+d\to e^++n+n$
3.25	5.99(−3)	5.92(−3)	6.46(−2)	
3.50	1.10(−2)	1.08(−2)	8.84(−2)	
3.75	1.79(−2)	1.77(−2)	1.16(−1)	
4.00	2.71(−2)	2.67(−2)	1.49(−1)	
4.25	3.88(−2)	3.81(−2)	1.86(−1)	1.37(−3)
4.50	5.32(−2)	5.22(−2)	2.28(−1)	5.98(−3)
4.75	7.05(−2)	6.92(−2)	2.75(−1)	1.37(−2)
5.00	9.11(−2)	8.92(−2)	3.27(−1)	2.47(−2)
5.25	1.15(−1)	1.13(−1)	3.85(−1)	3.89(−2)
5.50	1.43(−1)	1.39(−1)	4.47(−1)	5.72(−2)
5.75	1.74(−1)	1.70(−1)	5.16(−1)	7.95(−2)
6.0	1.83(−1)	1.79(−1)	5.89(−1)	1.06(−1)
6.5	2.51(−1)	2.44(−1)	7.53(−1)	1.71(−1)
7.0	3.32(−1)	3.21(−1)	9.40(−1)	2.54(−1)
7.5	4.26(−1)	4.12(−1)	1.15(0)	3.54(−1)
8.0	5.10(−1)	4.91(−1)	1.38(0)	4.73(−1)
8.5	6.24(−1)	5.99(−1)	1.64(0)	6.10(−1)
9.0	7.51(−1)	7.20(−1)	1.92(0)	7.65(−1)
9.5	8.93(−1)	8.53(−1)	2.22(0)	9.40(−1)
10.0	1.05(0)	1.00(0)	2.55(0)	1.13(0)
10.5	1.18(0)	1.12(0)	2.91(0)	1.35(0)
11.0	1.36(0)	1.29(0)	3.29(0)	1.58(0)
11.5	1.55(0)	1.47(0)	3.69(0)	1.83(0)
12	1.76(0)	1.66(0)	4.13(0)	2.09(0)
13	2.16(0)	2.03(0)	5.07(0)	2.69(0)
14	2.66(0)	2.48(0)	6.12(0)	3.36(0)
15	3.17(0)	2.94(0)	7.29(0)	4.10(0)
16	3.77(0)	3.48(0)	8.56(0)	4.91(0)
17	4.38(0)	4.02(0)	9.95(0)	5.84(0)
18	5.09(0)	4.64(0)	1.15(1)	6.80(0)
19	5.80(0)	5.27(0)	1.31(1)	7.84(0)
20	6.61(0)	5.97(0)	1.48(1)	8.94(0)
21	7.47(0)	6.71(0)	1.67(1)	1.01(1)

TABLE I. (*Continued*).

E_ν (MeV)	$\nu+d\rightarrow\nu'+n+p$	$\bar{\nu}+d\rightarrow\bar{\nu}'+n+p$	$\nu+d\rightarrow e^-+p+p$	$\bar{\nu}+d\rightarrow e^++n+n$
22	8.37(0)	7.48(0)	1.87(1)	1.14(1)
23	9.33(0)	8.29(0)	2.08(1)	1.27(1)
24	1.03(1)	9.14(0)	2.30(1)	1.41(1)
26	1.25(1)	1.09(1)	2.79(1)	1.70(1)
28	1.49(1)	1.29(1)	3.33(1)	2.03(1)
30	1.76(1)	1.50(1)	3.93(1)	2.38(1)
32	2.05(1)	1.73(1)	4.58(1)	2.75(1)
34	2.36(1)	1.98(1)	5.29(1)	3.15(1)
36	2.70(1)	2.23(1)	6.07(1)	3.57(1)
38	3.06(1)	2.51(1)	6.90(1)	4.02(1)
40	3.44(1)	2.79(1)	7.79(1)	4.49(1)
42	3.85(1)	3.09(1)	8.75(1)	4.98(1)
44	4.29(1)	3.41(1)	9.77(1)	5.49(1)
46	4.75(1)	3.74(1)	1.09(2)	6.02(1)
48	5.23(1)	4.08(1)	1.20(2)	6.58(1)
50	5.74(1)	4.43(1)	1.32(2)	7.15(1)
55	7.13(1)	5.36(1)	1.66(2)	8.66(1)
60	8.67(1)	6.37(1)	2.03(2)	1.03(2)
65	1.04(2)	7.43(1)	2.45(2)	1.20(2)
70	1.22(2)	8.56(1)	2.92(2)	1.38(2)
75	1.42(2)	9.73(1)	3.42(2)	1.56(2)
80	1.64(2)	1.09(2)	3.97(2)	1.75(2)
85	1.86(2)	1.22(2)	4.55(2)	1.95(2)
90	2.10(2)	1.35(2)	5.17(2)	2.15(2)
95	2.35(2)	1.48(2)	5.83(2)	2.35(2)
100	2.61(2)	1.61(2)	6.52(2)	2.55(2)
110	3.17(2)	1.88(2)	7.99(2)	2.96(2)
120	3.75(2)	2.15(2)	9.57(2)	3.37(2)
130	4.36(2)	2.42(2)	1.12(3)	3.77(2)
140	4.98(2)	2.68(2)	1.30(3)	4.17(2)
150	5.62(2)	2.94(2)	1.47(3)	4.56(2)
160	6.26(2)	3.19(2)	1.65(3)	4.94(2)

gle of the outgoing lepton, in terms of C_J, L_J, $T_J^{\rm el}$, and $T_J^{\rm mag}$, the charge, longitudinal electric, and magnetic projections of J_μ. For the conserved vector current L_J can be rewritten in terms of C_J. We also employ a generalized Siegert's theorem [8] to reexpress those components of $T_J^{\rm el}$ that are constrained by current conservation as multipoles of the charge operator. ($T_J^{\rm el}$ can be rewritten completely in terms of the charge operator only in the long-wavelength limit.) This application of the generalized Siegert's theorem is important because exchange current corrections to the charge operator are of relative order $(v/c)^2$, while those for the three-current are of relative order 1. The details of our treatment, including the matrix elements of the multipole operators, are given in Refs. [5,9].

As in Ref. [5], calculations have been performed for three realistic strong potentials, the Hamada-Johnson and those of the Paris and Bonn (OBEPR) groups. The results are in very good agreement apart from the tendency of the Bonn potential to give somewhat higher results for very low neutrino energies ($\sim 7\%$ at $E_\nu = 5$ MeV). In Table I we provide results for the Paris potential on a grid suitable for calculating charged- or neutral-current solar or stopped-muon-decay neutrino cross sections. In Table II we provide the ratio of the neutrino-induced to antineutrino-induced disintegration cross sections for the deuteron.

The averaged total cross sections over solar ^{8}B and ^{3}He$+p$ (hep) neutrinos from the Sun are

$$\langle\sigma\rangle_{^8\rm B} = \begin{cases} 4.44\times10^{-43}\ \text{cm}^2, & \nu_e+d\rightarrow\nu_e+n+p\ , \\ 1.15\times10^{-42}\ \text{cm}^2, & \nu_e+d\rightarrow e^-+p+p \end{cases}$$

and

$$\langle\sigma\rangle_{\rm hep} = \begin{cases} 1.24\times10^{-42}\ \text{cm}^2, & \nu_e+d\rightarrow\nu_e+n+p\ , \\ 2.97\times10^{-42}\ \text{cm}^2, & \nu_e+d\rightarrow e^-+p+p\ , \end{cases}$$

where an allowed β-decay spectrum has been used for hep neutrinos, and the distorting effects of the broad resonance populated in ^{8}B decay has been included in that calculation. These results are very similar to those given in YHH. For the standard solar model ^{8}B flux of $5.8\times10^6(1\pm0.37)/\text{cm}^2$ sec and a hep flux of $7.6\times10^3/\text{cm}^2$ sec, the corresponding rates for a 1 ktonne D_2O detector are

TABLE II. The ratios of ν and $\bar{\nu}$ cross sections for neutral- and charged-current breakup of deuterium as a function of the incident neutrino energy. These are Paris potential results.

E_ν (MeV)	$\sigma_{\nu\nu'}/\sigma_{\bar{\nu}\bar{\nu}'}$	$\sigma_{\nu e^-}/\sigma_{\bar{\nu}e^+}$
4	1.016	
6	1.016	5.569
8	1.038	2.920
10	1.049	2.252
15	1.077	1.778
20	1.108	1.657
30	1.169	1.654
40	1.233	1.737
50	1.297	1.850
70	1.428	2.118
90	1.558	2.407
110	1.684	2.700
130	1.802	2.980
150	1.910	3.235

$$R(^8\mathrm{B})=\begin{cases}4.9\times10^3/\mathrm{yr}, & \nu_e+d\to\nu_e+n+p\ ,\\ 1.3\times10^4/\mathrm{yr}, & \nu_e+d\to e^-+p+p\end{cases}$$

and

$$R(\mathrm{hep})=\begin{cases}18/\mathrm{yr}, & \nu_e+d\to\nu_e+n+p\ ,\\ 43/\mathrm{yr}, & \nu_e+d\to e^-+p+p\ .\end{cases}$$

Of course, these estimates ignore the reductions that would be associated with detector thresholds and efficiencies.

The results in Table I can also be folded with the neutrino flux distributions from supernovae. The precise spectral shapes for the electron and heavy-flavor neutrinos are still poorly known: only the electron antineutrinos from SN 1987A were observed. Yet, apart from an expected overestimation of the flux in the high-energy tail of the spectrum, it is believed that Fermi-Dirac distributions with temperatures ~4–5 MeV ($\nu_e,\bar{\nu}_e$) and ~8–10 MeV (ν_μ,ν_τ) are reasonable approximations to the true spectra [4]. Adopting the neutrino fluences (also used in Ref. [5])

$$\phi(\nu_e)=2.4\times10^{11}/\mathrm{cm}^2\left[\frac{8\ \mathrm{kpc}}{\mathrm{distance}}\right]^2,$$

$$\phi(\nu_\mu)=1.7\times10^{11}/\mathrm{cm}^2\left[\frac{8\ \mathrm{kpc}}{\mathrm{distance}}\right]^2,$$

$$\phi(\bar{\nu}_e)\sim0.7\phi(\nu_e)\ ,$$

$$\phi(\nu_\mu)=\phi(\bar{\nu}_\mu)=\phi(\nu_\tau)=\phi(\bar{\nu}_\tau)$$

and temperatures $T_{\nu_e}=T_{\bar{\nu}_e}=5$ MeV and $T_{\nu_\mu}=10$ MeV, we find that the total numbers of neutral-current and charged-current events in a 1-ktonne detector are

$$N^{\mathrm{NC}}=1.19\times10^3\left[\frac{8\ \mathrm{kpc}}{\mathrm{distance}}\right]^2,$$

$$N^{\mathrm{CC}}=0.26\times10^3\left[\frac{8\ \mathrm{kpc}}{\mathrm{distance}}\right]^2.$$

In an actual experiment these estimates will again be reduced by threshold and efficiency effects. The neutral-current results, which are dominated by the scattering of more energetic ν_μ and ν_τ neutrinos, would be more sharply affected by departures from a Fermi-Dirac distribution in the tail of the spectrum. For completeness, we note that the threshold for $\bar{\nu}_e+d\to n+n+e^+$ is just above the end-point energies of various terrestrial antineutrino sources, such as ^{214}Bi. (See, however, the recent discussion of Balantekin and Loreti on $\bar{\nu}_e$s generated from the solar-neutrino flux by interactions of neutrinos with the solar magnetic field [10].)

There are only a limited number of experimental tests of these cross sections. Deuteron photodisintegration tests the calculated vector current responses, and has been studied by Ying, Henley, and Miller and many other authors previously [11]. One direct test of the full weak response is the measurement by Willis *et al.* [12] of the total cross section for $\nu_e+d\to e^-+p+p$ following the decay of stopped muons in the LAMPF beamstop. The normalized ν_e distribution

$$\phi(\nu_e)=\frac{192}{m_\mu^4}E_{\nu_e}^2\left[\frac{m_\mu}{2}-E_{\nu_e}\right]$$

has an end point of $m_\mu/2$ and is maximal at $E_{\nu_e}\sim40$ MeV. Thus this flux resembles that expected for heavy-flavor supernova neutrinos ($\langle E_{\nu_\mu}\rangle\sim3.15T_{\nu_\mu}\sim25$ MeV). This "calibration" is also interesting because first-forbidden responses become important at these inter-

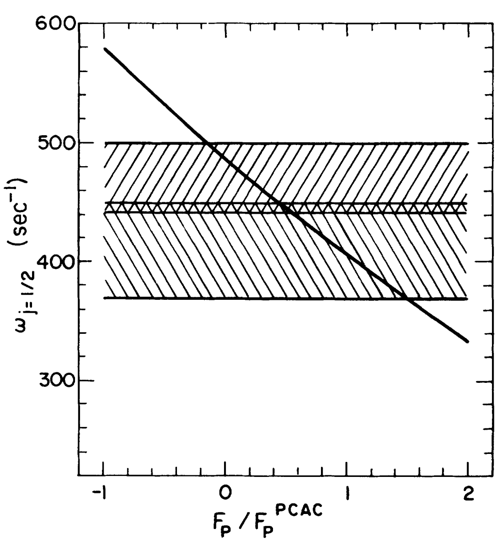

FIG. 1. Dependence of the $j=\frac{1}{2}$ hyperfine muon-capture rate on the pseudoscalar form factor F_P. The upper shaded band corresponds to the value obtained in Ref. [15] and the lower shaded band corresponds to the value obtained in Ref. [16]. An amount of 30 sec^{-1} is added to our numerical value, in order to account for the two-body contributions [14], so that a comparison to experimental data can be made.

TABLE III. Ratio of the Paris potential cross section of Doi and Kubodera [7] to those of this paper.

E_ν (MeV)	$\nu+d\to\nu'+n+p$	$\bar{\nu}+d\to\bar{\nu}'+n+p$	$\nu+d\to e^-+p+p$	$\bar{\nu}+d\to e^++n+n$
4	1.11	1.11	1.04	
6	1.08	1.08	1.04	1.18
8	1.07	1.07	1.04	1.10
10	1.03	1.03	1.04	1.08
20	1.04	1.03	1.04	1.05
80	0.99	0.99	1.00	1.01
100	0.99	0.98	0.99	1.01
150	1.01	0.99	1.02	1.03

mediate energies. Our cross sections yield

$$\langle \sigma \rangle_{\text{stop}\,\nu_e\,\text{flux}} = 0.53\times 10^{-40}\ \text{cm}^2$$

which is in excellent agreement with the experimental value [12]

$$\langle \sigma \rangle = (0.52\pm 0.18)\times 10^{-40}\ \text{cm}^2\ .$$

It seems to us that a remeasurement of this cross section to obtain a more precise value would be quite valuable.

A second test is provided by hyperfine $j=\frac{1}{2}$ muon-capture rate (the $j=\frac{3}{2}$ rate is quite suppressed). While this process tests the nuclear response for timelike q_μ^2, rather than the spacelike q_μ^2 encountered in the scattering processes, it is also true that most of the capture rate is due to the same "giant resonances" that play a role in first-forbidden neutrino cross sections.

The calculation was performed by assuming that the initial muon is in the first Bohr orbit of a pointlike deuteron. While details of the calculation will be given elsewhere [9], we do need to stress that our results are affected by the uncertainty in the value of the pseudoscalar coupling F_P. While the usual Goldhaber-Treiman argument gives the partial-conservation-of-the-axial-current (PCAC) value, $F_P/F_A \sim 7/m_\pi$ for $q^2 \approx -m_\pi^2$, values almost twice as large have been deduced from studies of axial-charge μ-capture and β-decay transitions in light- and medium-mass nuclei [13]. Adopting the PCAC value we obtain the Paris potential rate $\omega^{\text{1-body}} = 361/\text{sec}$, a value in excellent agreement with the Reid soft core (365/sec) and Paris (369/sec) potential 1-body results of TKK [6]. Previous estimates of exchange current corrections, which we have not included apart from the model-independent contributions taken from Siegert's theorem, have increased rates by about 30/sec [6,14]. Thus our result is in reasonable agreement with two experimental determinations (470±29/sec [15] and 409±40/sec [16]) though the difference in the central values of those measurements is considerable. In Fig. 1 the theoretical rate is compared to experiment as a function of F_P.

Perhaps the most important check on our work is provided by independent calculations of Doi and Kubodera. As discussed in the Introduction, there exist two calculations in the literature that retain N-N relative partial waves other than s waves and that therefore might be valid at the higher energies of interest for supernova or muon-decay neutrinos. The first was our previous effort (YHH) in which a coding error in the $J=1$ magnetic projection of the axial current led to the corresponding first-forbidden matrix element being a factor of 2 too large. The second is the calculation of Tatara, Kohyama, and Kubodera where terms of order $|\mathbf{J}^V|^2$ were dropped, where $\mathbf{J}^V$ is the vector three-current, so that the transverse vector response of the nucleus was neglected. In this paper our coding error has been corrected, and in the accompanying paper by Doi and Kubodera the full transverse response has been calculated. Thus it is of great interest to see how the two improved calculations now compare.

The agreement between the results is very good, certainly within a range consistent with differences due to exchange currents, strong potential choices (including charge-independence-breaking effects), and alternative prescriptions for imposing the constraints of current conservation. In Table III a detailed comparison is given, demonstrating that the Doi and Kubodera results typically agree with ours to about 5%, a discrepancy that is reasonable to attribute to exchange currents and minor technical differences in the calculations. (The latter are detailed in Ref. [5].)

This comparison, the results for the LAMPF cross section and muon-capture rates, and the demonstration of the insensitivity to the choice of strong potential all suggest that the various cross sections are understood to an accuracy of about 10%. This is clearly of great importance to the interpretation of future results from SNO.

We thank K. Kubodera and M. Doi for discussions and for sharing results that helped us locate the error in Ref. [5]. This work was supported in part by the U. S. Department of Energy and by NASA under Grant No. NAGW-2523.

[1] G. T. Ewan *et al.*, Sudbury Neutrino Observatory Proposal No. SNO-87-12 (1987).

[2] S. P. Mikheyev and A. Yu. Smirnov, Yad. Fiz. **42**, 1441 (1985) [Sov. J. Nucl. Phys. **42**, 913 (1985)]; Nuovo Cimento **9C**, 17 (1986); L. Wolfenstein, Phys. Rev. D **17**, 2369 (1978); **20**, 2634 (1979).

[3] J. N. Bahcall, K. Kubodera, and S. Nozawa, Phys. Rev. D **38**, 1030 (1988); H. C. Lee, Nucl. Phys. **A294**, 473 (1978); S. D. Ellis and J. N. Bahcall, *ibid.* **A114**, 636 (1968); F. T. Avignone III, Phys. Rev. D **24**, 778 (1981); T. Ahrens and L. Gallaher, *ibid.* **20**, 2714 (1979); A. Aliand and C. A. Dominguez, *ibid.* **12**, 3673 (1975); W. Müller and M. Gari, Phys. Lett. **102B**, 389 (1981).

[4] See, for example, R. W. Mayle, J. R. Wilson, and D. W. Schramm, Astrophys. J. **318**, 288 (1987).

[5] S. Ying, W. C. Haxton, and E. M. Henley, Phys. Rev. D **40**, 3211 (1989).

[6] N. Tatara, Y. Kohyama, and K. Kubodera, Phys. Rev. C **42**, 1694 (1990).

[7] M. Doi and K. Kubodera, Phys. Rev. C **45**, 1988 (1992), this issue.

[8] J. L. Friar and S. Fallieros, Phys. Rev. C **29**, 1645 (1984); A. J. F. Siegert, Phys. Rev. **52**, 787 (1937).

[9] S. Ying and E. M. Henley, private communication.

[10] A. B. Balantekin and F. Loreti, Phys. Rev. **D45**, 1059 (1992).

[11] S. Ying, E. M. Henley, and G. A. Miller, Phys. Rev. C **38**, 1584 (1988); J. L. Friar, in *Perspectives in Nuclear Physics at Intermediate Energies,* edited by S. Boffi, C. Ciofi degli Atti, and M. M. Giannini (World Scientific, Singapore, 1984), p. 124, and references therein.

[12] S. E. Willis *et al.*, Phys. Rev. Lett. **44**, 522 (1980).

[13] Some of the determinations are summarized by I. S. Towner, Annu. Rev. Nucl. Part. Sci. **36**, 115 (1986); also see W. C. Haxton and C. Johnson, Phys. Rev. Lett. **65**, 1325 (1990); S. Nozawa, K. Kubodera, and H. Ohtsubo, Nucl. Phys. **A453**, 645 (1986).

[14] E. Ivanov and E. Truhlik, Nucl. Phys. **A316**, 451 (1979).

[15] G. Bardin, J. Duclos, J. Martino, A. Bertin, M. Capponi, M. Piccinini, and A. Vitale, Nucl. Phys. **A453**, 591 (1986).

[16] M. Cargnelli, dissertation, Universität Wien, 1987; M. Marton, P. Pawlek, J. Werner, J. Zmeskal, W. Bertle, and C. Petitjean, in *Proceedings of the XXIII Yamada Conference on Nuclear Weak Processes and Nuclear Structure,* Osaka, 1989, edited by M. Morita, H. Ejiri, H. Ohtsubo, and T. Suto (World Scientific, Singapore, 1989), p. 115.